CHIN. PHYS. LETT. Vol. 26, No. 8 (2009) 086802

A Thin Liquid Film and Its Effects in an Atomic Force Microscopy Measurement *

LIN Jing(林静)[1,2**], ZHENG Zhi-Jun(郑志军)[2], YU Ji-Lin(虞吉林)[1], BAI Yi-Long(白以龙)[2]

[1]*CAS Key Laboratory of Mechanical Behavior and Design of Materials, University of Science and Technology of China, Hefei 230027*

[2]*State Key Laboratory of Nonlinear Mechanics, Institute of Mechanics, Chinese Academy of Sciences, Beijing 100190*

(Received 28 April 2009)

Recently, it has been observed that a liquid film spreading on a sample surface will significantly distort atomic force microscopy (AFM) measurements. In order to elaborate on the effect, we establish an equation governing the deformation of liquid film under its interaction with the AFM tip and substrate. A key issue is the critical liquid bump height y_{0c}, at which the liquid film jumps to contact the AFM tip. It is found that there are three distinct regimes in the variation of y_{0c} with film thickness H, depending on Hamaker constants of tip, sample and liquid. Noticeably, there is a characteristic thickness H^* physically defining what a thin film is; namely, once the film thickness H is the same order as H^*, the effect of film thickness should be taken into account. The value of H^* is dependent on Hamaker constants and liquid surface tension as well as tip radius.

PACS: 68.08.De, 68.37.Ps

The invention of atomic force microscopy (AFM)[1,2] has enabled us to observe material behavior and surface topography at nano scales. Without the restriction of operating in a vacuum environment, AFM has been increasingly used to study surface topography as well as the mechanical properties of various samples, especially soft matter such as polymers and biological samples.[3,4] Hence, it is significant to fully understand the interaction between the AFM probe and sample in AFM measurement; namely, the deflection of the AFM cantilever induced by the interaction between tip and sample should truly reflect the surface topography and mechanical properties of the sample.[5]

However, in ambient air, a liquid film may appear on sample surface. The film will interact with the AFM tip, and then affect the deflection of the cantilever leading to distorted force signals.[6] In order to obtain the genuine surface topography and mechanical properties of the sample from the AFM measurement data, it is necessary to understand the effect of liquid film on the interaction between the AFM tip and sample in details.

To understand the effect of liquid film in AFM tests, many researchers have conducted various studies.[7–9] Theoretically, the total energy of the system consists of the liquid surface energy $W_\gamma(y)$, gravitational potential of the mass of liquid bump $W_g(y)$ and the energy related to the van der Waals interaction between the tip and the liquid $W_{vdW}(y)$, where $y(r)$ is the axisymmetrical shape of the liquid bump. By minimizing the total energy functional with respect to the shape function $y(r)$, previous work obtained the equation governing the surface deformation of a semi-infinite liquid.[8] Obviously, the semi-infinite liquid model is unable to unveil the film thickness effects appearing in most AFM measurements. Hence, following the aforementioned energy approach, some researchers developed a similar equation for liquid film. Unfortunately, the obtained equation failed to degenerate to its semi-infinite counterpart,[7] indicating something wrong there. In this Letter, we establish a new equation governing the surface deformation of liquid film and have the equation cross-checked by means of both energy minimization and force balance. Then, we analyze the deformation of liquid film under its interaction with the AFM tip. A key scale in the phenomenon is the critical liquid bump height y_{0c}, at which the liquid film jumps up to touch the AFM tip. Generally speaking, the critical bump height y_{0c} in the case of a finite thickness film remains in the same order as that of a semi-infinite liquid. More specifically, there are three distinct regimes of the variation of y_{0c} with film thickness H, depending on the difference of Hamaker constant between sample and liquid. In particular, we find a characteristic thickness H^* of liquid film. Provided that the film thickness H is the same order as H^*, the effect of film thickness will become quite considerable.

Due to the flowability of liquids, the film will no longer remain stable under its interaction with the tip. As shown in Fig. 1, we analyze the deformation of a thin liquid film on a substrate under the interaction of a spherical tip with radius R, as in earlier investigations. The forces involved in the system consist of four parts: the surface tension forces of the deformed

*Supported by National Natural Scientific Foundation of China under Grant Nos. 10721202, 10432050, 10772012, 10732090, and the Knowledge Innovation Project of Chinese Academy of Sciences (KJCX2-YW-M04).

**Email: linjing@mail.ustc.edu.cn

liquid film F_γ, gravity G_1 and G_2 of the deformed and unperturbed liquid film, the van der Waals force between tip and liquid F_{sp-l} and the van der Waals force between tip and sample F_{sp-s}. All the forces are a function of the liquid surface shape $y(r)$. The balance of all forces of the system leads to the following equation, as shown in Fig. 1,

$$F_{sp-l} + F_{sp-s} = G_1 - G_2 + F_\gamma^1, \tag{1}$$

where F_γ^1 is the surface tension force of the deformed liquid film F_γ along the vertical direction.

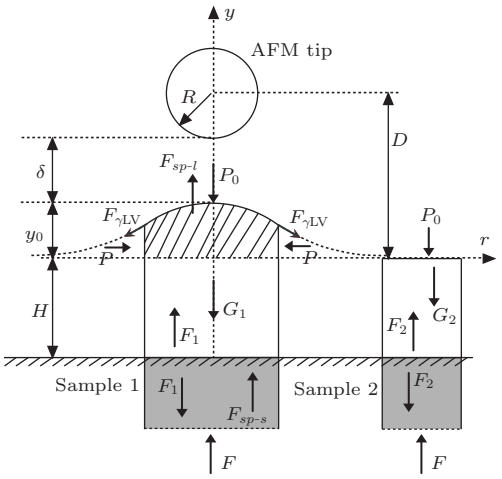

Fig. 1. A sketch showing the deformation of the liquid film surface under its interaction with a sphere tip and an analysis of force balancing. F_1 and F_2 are the interactions between the sample and liquid film at two locations, F_γ is the surface tension force of the deformed liquid film, G_1 and G_2 are the gravities of the deformed and unperturbed liquid films, F_{sp-l} and F_{sp-s} are the van der Waals between tip and liquid and between tip and sample respectively, P_0 is the atmospheric pressure, and F is the supporting force of the far field sample.

Based on the van der Waals attractive potential,[10] the forces F_{sp-l} and F_{sp-s} can be expressed as

$$F_{sp-l} = \frac{4A_{sp-l}R^3}{3\pi}\int_0^r \{-[(D+H)^2 + r^2 - R^2]^{-3} + [(D-y)^2 + r^2 - R^2]^{-3}\} \cdot 2\pi r dr, \tag{2}$$

$$F_{sp-s} = \frac{4A_{sp-s}R^3}{3\pi}\int_0^r [(D+H)^2 + r^2 - R^2]^{-3} \cdot 2\pi r dr, \tag{3}$$

where A_{sp-l} and A_{sp-s} are Hamaker constants between tip and liquid and between tip and sample respectively, D is the distance between the center of the sphere tip and the unperturbed liquid surface, see Fig. 1. The vertical force resulting from surface tension of the deformed liquid film F_γ^1 can be expressed as[11]

$$F_\gamma^1 = \gamma_{LV}\big(-y'(1+y'^2)^{-1/2}\big) \cdot 2\pi r, \tag{4}$$

where γ_{LV} is surface tension coefficient of the liquid. The gravity $G_1 - G_2$ can be obtained from the volume integral of the deformed and unperturbed liquid films as follows:

$$G_1 - G_2 = \rho g \int_0^r y \cdot 2\pi r dr, \tag{5}$$

where ρ is the liquid density and g is the gravitational acceleration.

After combining these equations, we deduce the equation governing the shape of the liquid surface $y(r)$ as follows:

$$\frac{1}{r}\frac{d}{dr}\left[\frac{ry'}{\sqrt{1+y'^2}}\right] - \frac{\rho g y}{\gamma_{LV}} + \frac{4A_{sp-l}R^3}{3\pi\gamma_{LV}} \cdot \left[(D-y)^2 + r^2 - R^2\right]^{-3} + \frac{4(A_{sp-s} - A_{sp-l})R^3}{3\pi\gamma_{LV}} \cdot \left[(D+H)^2 + r^2 - R^2\right]^{-3} = 0, \tag{6}$$

together with the axisymmetric condition $y'(0) = 0$ and far field condition $\lim_{r\to\infty} y(r) = 0$. We also derive Eq. (6) by minimization of the total energy of the system with additional consideration of the liquid-sample interface deformation (compared to previous work[7]) and justify the governing equation (6) as valid.

Supposing that A_{sp-s} is equal to A_{sp-l}, Eq. (6) is reduced to

$$\frac{1}{r}\frac{d}{dr}\left[r\frac{y'}{(1+y'^2)^{1/2}}\right] + \frac{4AR^3}{3\pi\gamma_{LV}}\left[(D-y)^2 + r^2 - R^2\right]^{-3} - \frac{\rho g y}{\gamma_{LV}} = 0, \tag{7}$$

which is the same as the equation of semi-infinite liquid obtained previously.[7,8]

To obtain an analytic representation of the liquid surface, we apply the same perturbation method to Eq. (6) as used in the previous works;[8,12] the height of the liquid bump apex $y_0 = y(r=0)$ can be expressed as

$$y_0 = \frac{(A_{sp-s} - A_{sp-l})}{3\pi\gamma_{LV}}\frac{R^3}{[(D+H)^2 - R^2]^2} \cdot \left(\frac{1}{2} + \ln\frac{2\lambda}{\sqrt{(D+H)^2 - R^2}} - Eu\right) + \frac{A_{sp-l}}{3\pi\gamma_{LV}}\frac{R^3}{[(D-y_0 t)^2 - R^2]^2} \cdot \left(\frac{1}{2} + \ln\frac{2\lambda}{\sqrt{(D-y_0)^2 - R^2}} - Eu\right), \tag{8}$$

where $\lambda = \sqrt{\gamma_{LV}/\rho g}$, and $Eu \approx 0.57721$ is Euler's constant.

The numerical results of the governing equation (6), obtained by means of shooting methods, i.e. the Runge–Kutta–Fehlberg method with adaptive step size control, are shown in Fig. 2. In order to compare with experimental results, the parameters used in our computations are adopted according to the corresponding experiment: $R = 220\,\text{nm}$, $H = 10\,\text{nm}$,

$\rho = 1.8 \times 10^3\,\mathrm{kg/m^3}$, $g = 9.8\,\mathrm{m/s^2}$, $\gamma_{\mathrm{LV}} = 0.021\,\mathrm{N/m}$, $A_{sp-l} = 1.31 \times 10^{-19}\,\mathrm{J}$ and $A_{sp-s} = 0.81 \times 10^{-19}\,\mathrm{J}$. When the AFM tip approaches the liquid surface, namely with deceasing distance D, the height of the bump $y_0 = y(0)$ gradually increases until a critical tip-liquid distance D_c, at which the liquid surface is unable to remain stable and will jump up to touch the probe tip. Figure 3 illustrates a rapid y_0 increase with a small deceasing D at the critical distance. When the tip moves to the critical distance $D_c = 1.0614R$ in the case shown in Fig. 3, the liquid surface is going to jump to the probe.

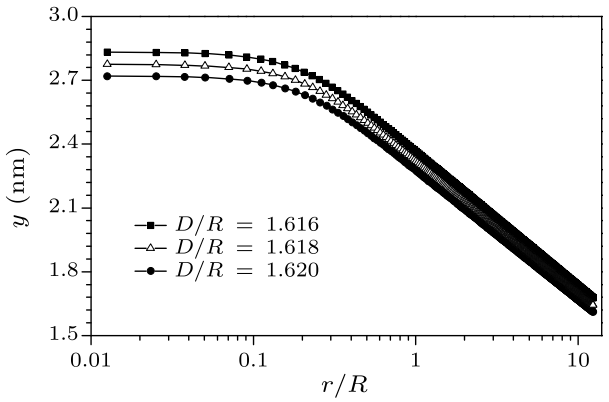

Fig. 2. Dimensionless shape of liquid bump at different tip-liquid distances D.

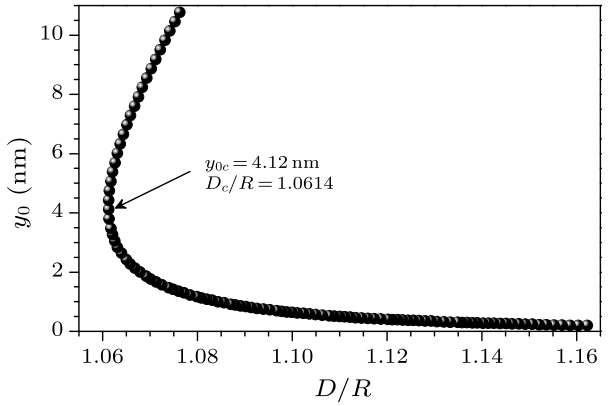

Fig. 3. Variation of liquid bump apex y_0 with tip-liquid distance D and critical tip-liquid distance D_c, i.e. the jump-to-contact point.

Beyond this point, there is no stable liquid bump unless the liquid surface touches the tip. Therefore we can take

$$dy_0/(-dD) \to \infty, \tag{9}$$

as the critical condition of the jump-to-contact and D_c can be determined by Eq. (8) and the critical condition (9). By assuming tip wetting occurring at this critical condition, the apparent film thickness will present an offset $\Delta H = D_c - R = y_{0c} + \delta_c$, where y_{0c} and δ_c are the critical bump apex height and the gap between tip and bump. For a given liquid, tip and sample, the jump-to-contact distance D_c depends on the film thickness H.

In order to verify our model, we compared our results of the apparent film thickness $H + \Delta H$ with previous experimental measurements. In our calculations of Figs. 2 and 4, we took the same physical parameters as those parameters in the experiment.[7] Figure 4(a) shows the two apparent thicknesses $H + \Delta H$ of liquid film measured by AFM[7] and calculated with our model respectively, against the thickness H of the undisturbed virgin film. Clearly, there is a reasonable agreement between our calculations and the experimental results, and the presence of an offset in film thickness with both theoretical and experimental approaches is apparent. However, the Hamaker constant difference almost has no influence on it, except that the thickness H goes down to a few nanometers as shown in Fig. 4(b). This offset indicates that the wetting of the tip occurs before the tip can touch the undisturbed liquid surface.

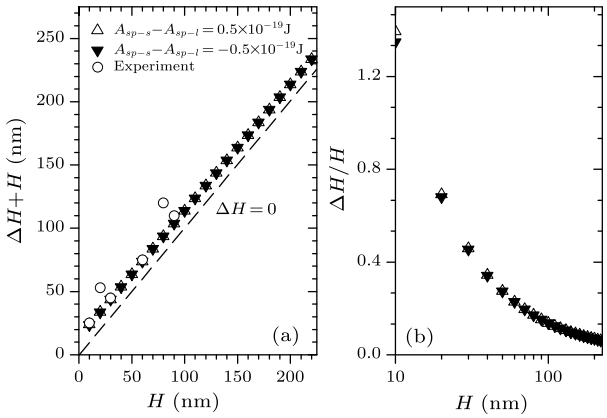

Fig. 4. (a) Apparent film thickness $H + \Delta H$ measured with AFM[7] and calculated in terms of offset $\Delta H = D_c - R = y_{0c} + \delta_c$ with two Hamaker constant differences $A_{sp-s} - A_{sp-l}$ versus the reference thicknesses H, experimentally measured with an ellipsometric.[7] (b) The ratio of offset and reference thicknesses $\Delta H/H$ with the same Hamaker constant difference $A_{sp-s} - A_{sp-l}$ versus the reference thicknesses H.

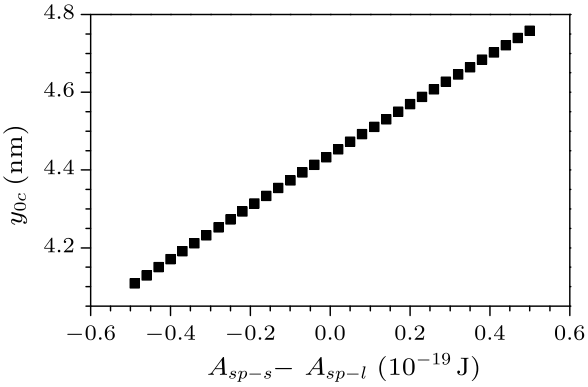

Fig. 5. Critical height of liquid bump apex y_{0c} increases with increasing Hamaker constant difference $A_{sp-s} - A_{sp-l}$ at a fixed film thickness $H = 10\,\mathrm{nm}$.

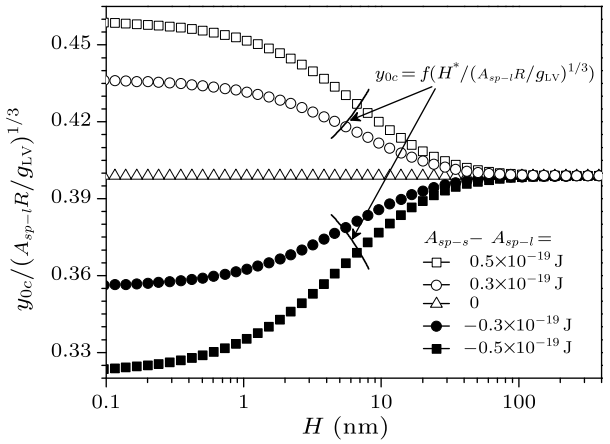

Fig. 6. Three regimes of the critical bump apex height dimensionless y_{0c} with dimensionless film thickness H in the three ranges of Hamaker constant difference $A_{sp-s} - A_{sp-l}$, where H^* with various Hamaker constant differences is of the order that the film thickness H has an apparent influence on the critical height y_{0c}.

Because of the significance of the critical height of the liquid bump y_{0c}, we take a close look at the critical phenomenon. Firstly, for a semi-infinite liquid, it is obvious from Eq. (8) that the greater the Hamaker constant between tip and liquid with a fixed surface energy γ_{LV}, the greater the critical height y_{0c} and the critical distance D_c, indicating the system is more prone to the critical jump to contact. Thus, for a film on a substrate with $A_{sp-s} - A_{sp-l} > 0$, the equivalent Hamaker constant of the system becomes greater than that of the semi-infinite liquid, leading to a greater critical height y_{0c} at a fixed thickness H as shown in Fig. 5. According to Eq. (8), when the order of the first term is equal to the second, the variations of film thickness H will apparently influence the critical height y_{0c}. In this situation, the order of film thickness H is characterized by

$$H^* = \sqrt{\frac{|A_{sp-s} - A_{sp-l}|}{A_{sp-l}}} \left(\frac{A_{sp-l}R}{\gamma_{LV}}\right)^{1/3}. \qquad (10)$$

As shown in Fig. 6, the critical height of the liquid bump may become independent of film thickness H, provided that the thickness of the virgin liquid film is much bigger than H^*. Only when the film thickness H is comparable with H^* will the film deformation vary with film thickness H, and the liquid film should be regarded as a thin film and has an influence on the liquid deformation. However, the critical bump apex height y_{0c} almost always remains of the order $(A_{sp-l}R/\gamma_{LV})^{1/3}$, i.e. the same as the semi-infinite liquid.[8] Hence, the Hamaker constant between tip and substrate A_{sp-s} and film thickness H have a secondary influence on the critical height y_{0c}. When paying more attention to detail, we find that the variations of y_{0c} with film thickness H in different ranges of Hamaker constant difference $A_{sp-s} - A_{sp-l}$ show three regimes, see Fig. 6. When $A_{sp-s} - A_{sp-l} < 0$, the critical height of the liquid bump y_{0c} increases with increasing thickness H, whereas y_{0c} decreases if $A_{sp-s} - A_{sp-l} > 0$. The mechanism underlying the effect is in agreement with the previous understanding of the increasing critical height y_{0c} with increasing Hamaker constant difference $A_{sp-s} - A_{sp-l}$ in Fig. 5. When the film is thick enough, these two curves of y_{0c} merge with each other and y_{0c} reaches the value at $A_{sp-s} - A_{sp-l} = 0$, namely the semi infinite liquid.

Based on the above analyses and relevant material parameters, we may have to consider not only the interaction between the sample and tip but also the effect of liquid film on AFM measurement in conventional operations in the laboratory, namely nanometer-thick liquid film on sample.

In summary, we have presented the governing equation and analysis of the deformation of liquid film on a sample. The calculated offset of film thickness based on the analysis shows reasonable agreement with the previous AFM measurement. In fact, the critical height of the liquid bump y_{0c} at jump-to-contact plays a key role in the measurement and is dependent on film thickness, Hamaker constants, surface tension as well as probe tip radius. In particular, if the liquid film thickness H is the same order as the critical thickness $\sqrt{|A_{sp-s} - A_{sp-l}|/A_{sp-l}}(A_{sp-l}R/\gamma_{LV})^{1/3}$, the film thickness must be taken into account. For different Hamaker constant differences $A_{sp-s} - A_{sp-l} < 0$ or > 0, the critical height of the liquid bump y_{0c} shows increasing or decreasing variation with increasing film thickness H. These findings are helpful to understand the influence of liquid film in AFM measurements.

References

[1] Binnig G, Rohrer H, Gerber C and Weibel E 1982 *Appl. Phys. Lett.* **40** 178
[2] Binnig G, Quate C F and Gerber C 1986 *Phys. Rev. Lett.* **56** 930
[3] Zitzler L, Herminghaus S and Mugele F 2002 *Phys. Rev.* B **66** 155436
[4] Landman U, Luedtke W D, Burnham N A and Colton R J 1990 *Science* **248** 454
[5] Wang HY, Ming H, Liu N, Xia M F, Ke F J and Bai Y L 2007 *Chem. Eng. Sci.* **62** 3589
[6] Cappella B and Dietler G 1999 *Surf. Sci. Rep.* **34** 1
[7] Forcada M L, Jakas M M and Grasmarti A 1991 *J. Chem. Phys.* **91** 706
[8] Liu N, Bai Y L, Xia M F and Ke F J 2005 *Chin. Phys. Lett.* **22** 2012
[9] Li X D and Peng Y 2006 *Appl. Phys. Lett.* **89** 234104
[10] Israelachvili J N 1985 *Intermolecular and Surface Forces* (London: Academic)
[11] Forcada M L, Arista N R and Alberto G M 1991 *Phy. Rev.* B **44** 8226
[12] Nayfeh A H 1981 *Introduction to Perturbation Techniques* (New York: Academic)